Proceedings of the 28th IEEE
EMBS Annual International Conference
New York City, USA, Aug 30-Sept 3, 2006

Biocompatible MEMS Electrode Array for Determination of Three-Dimensional Strain

Boyd M. Evans III, *Student Member, IEEE;* Mohamed R. Mahfouz, *Senior Member, IEEE*;
Emily R. Pritchard, *Student Member, IEEE*

***Abstract*—Sensor arrays for the measurement of the load condition of polyethylene spacers in the total knee arthroplasty (TKA) prosthesis have been developed. Arrays of capacitive sensors are used to determine the three-dimensional strain within the polyethylene prosthesis component. Data from these sensors can be used to give researchers better understanding of component motion, loading, and wear phenomena for a large range of activities. These sensors implemented on a large scale will give clinicians feedback for individual patient biomechanics without the requirement for patient exposure to x-ray radiation. Patients will benefit from smart prosthetic components which allow clinicians monitor biomechanics and loading by applying noninvasive remedies such as orthotics or physical therapy for patients exhibiting poor biomechanics before wear or component failure become issues. In this paper, we present research regarding the design of a biocompatible strain sensor and the fabrication of microelectrode arrays on biocompatible polymer materials.**

I. Introduction

THE annual number of total knee arthroplasty procedures in the United States has been reported to be more than 326,000 per year by the National Inpatient Survey (NIS) of medical procedures [1]. The proportion of revisions (surgery to replace a failed knee replacement joint) to primary (first joint replacement) procedures is reported to be 8-15% of total procedures [2]. The longevity of these implants varies significantly in published literature, from 8-20 years [3]. Due to undesirable revision rates and increased implant performance demands, the need exists for further understanding of the loads and mechanics of knee replacement components.

Instrumentation of orthopedic implants in humans has been performed by a few researchers on a small number of patients. Initial research pertaining to instrumented orthopedic components was performed on instrumented hips by Nils Rydell, who gathered a significant amount of data regarding the muscle loading of the hip in his study using strain gauges and leads passing through the skin [4]. Bergmann extended the work of Rydell through the use of telemetry, an inductive power supply, and strain gauges. Bergmann reported loads from two patients. His data showed that joint loads range from 2.8 to 4.8 times body weight (BW) depending on walking speeds [5]. Researchers at the Scripps Clinic have recently published information on an instrumented tibial tray with similar results [6].

Just as significant as total component load, the relative implant kinematics, contact areas, and contact stresses are critical to the performance and wear of any prosthesis. Maximum contact pressures between metal components and a polyethylene inserts have been reported to approach the yield strength of polyethylene (approximately 20 MPa) in knee replacements and 7 MPa for hip replacement prosthesis by researchers using finite element modeling, Fuji pressure sensitive film, and cadaver studies [7], [8]. Researchers Komistek and Mahfouz have used video fluoroscopy to track the implant motions including the contact points of knee, hip, and shoulder replacements [9]. Our goal is to extend this work by developing microelectromechanical sensors (MEMS) capable of determining the contact pressure and area plus the contact motions with minimal modification of existing biomedical components.

Fig. 1. Components in total knee replacement prosthesis. Components replace diseased joint surfaces.

Manuscript received April 3, 2006.

Boyd M. Evans is with the University of Tennessee, Department of Mechanical, Aerospace, and Biomedical Engineering, 301 Perkins Hall, Knoxville, TN 37996 (phone: 865-574-9418; fax: 865-946-1787; e-mail: ev3@cmb.utk.edu).

Mohamed R. Mafouz is with the University of Tennessee, Department of Mechanical, Aerospace, and Biomedical Engineering, 213 Perkins Hall, Knoxville, TN 37996 (phone: 865-974-7668; fax: 865-946-1787; e-mail: mmahfouz@ utk.edu)

Emily R. Pritchard is with the University of Tennessee, Department of Mechanical, Aerospace, and Biomedical Engineering, 301 Perkins Hall, Knoxville, TN 37996 (phone: 865-974-2093; fax: 865-946-1787; e-mail: epritchard@cmb.utk.edu).

This work was performed in part at the Cornell NanoScale Facility, a member of the National Nanotechnology Infrastructure Network, which is supported by the National Science Foundation (Grant ECS 03-35765).

II. Materials and Methods

A. Sensor Geometry

We have investigated the use of three different sensors to determine the normal forces, in-plane forces, and shear forces. A prototype element of this sensor is shown in Fig. 2. To fully characterize the strain tensor in three dimensions, six sensors are required to solve for the three normal strains and three shear strains. More detail about the function of these sensors is shown in Fig. 3. A parallel plate capacitor is used to determine the strain normal to the plane of the sensors, ε_{zz}. Two differential translating capacitors indicate the shear components normal to the sensor plane, ε_{zx} and ε_{zy}. Three interdigitated capacitors function to determine ε_{xx}, ε_{yy}, and ε_{xy}.

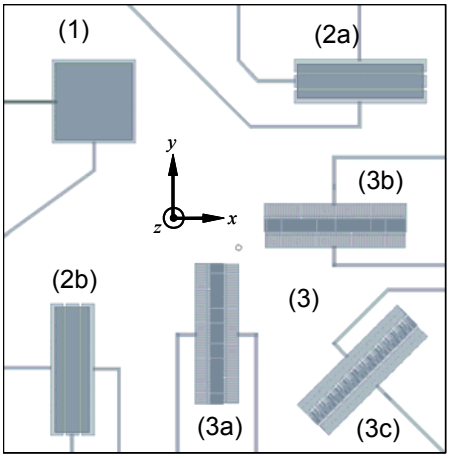

Fig. 2. Planar multiaxial strain sensor, with elements for z direction strain (1), xz shear (2a), yz shear, (2b), x strain (3a), y strain (3b), and xy shear (3c).

Element 1 in Fig. 2 and Fig. 3, determines the strain normal to the plane of the sensing element. For the simple case of strain normal to the sensor plane, the relationships coupling stress, strain, and capacitance are shown in (1)-(3), C represents the capacitance, d is the gap distance, A is the area of the capacitor, ε_r is the relative permittivity of the dielectric material, ε_0 is the permittivity of free space, s represents strain, and E is the elastic modulus. For the parallel plate capacitor, the change in distance between the plates is the response to the strain mechanism and occurs in the direction shown in Figure 3.

$$\frac{dC}{dl} = -\frac{\varepsilon_r \varepsilon_0 A}{l^2} \tag{1}$$

$$s \approx -\frac{\Delta C l_0}{\varepsilon_r \varepsilon_0 A} \tag{2}$$

$$\sigma \approx -\frac{\Delta C l_0 E}{\varepsilon_r \varepsilon_0 A} \tag{3}$$

Element two in Fig. 2 and Fig. 3 is a differential capacitor used to measure the shear strain in the material.

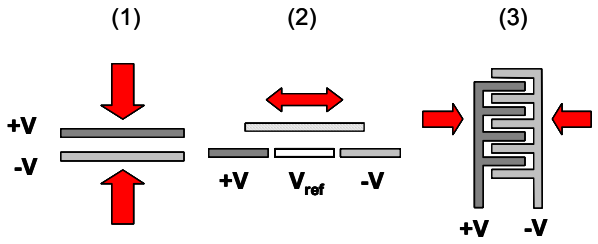

Fig. 3. Two dimensional illustrations of sensor capacitance function. Electrode configuration and direction of sensitivity are displayed.

The differential geometry used for the shear sensor has the ability to cancel out unwanted effects. A voltage is applied between the two outer electrodes labelled +V and –V, the upper electrode is electrically floating, and the center electrode, V_{ref}, indicates the measurement. This arrangement has zero signal when it is balanced and motion of the upper plate relative to the lower ones yields a signal which has a sign indicating the direction of motion. The upper plate which is at floating potential acts as a moving dielectric in this arrangement. Motion of the upper electrode in any direction other than the sensing direction results in no signal, because the effect is seen equally by both capacitors. The equation relating the change in capacitance with the change in strain is shown below, where w is the width of the electrode, τ is the shear stress, G is shear modulus, and γ is shear strain.

$$\tau = \frac{G\Delta C}{\varepsilon_r \varepsilon_0 w} \tag{4}$$

Sensor element three of Figure 3 is an interdigitated capacitor design. As this element experiences strain, several effects may be present, such as transverse strain characterized by Poisson's ratio. In this paper, we investigate the effects of that loading situation and the optimization of the geometry to minimize those effects. For a thin-film sensor the capacitance has a large fringe component and is approximated by (5) and (6). In these equations, K and K' represent elliptical integrals of the first kind of k and k', a is the distance between digits, b is the digit width. ε_s and ε_p are the relative permittivity constants of the substrate and polymer material coating capacitor.

$$k = \frac{a}{a+b},\ k' = \sqrt{1-k^2} \tag{5}$$

$$C = \varepsilon_0 \frac{(\varepsilon_s + \varepsilon_p)}{2} \frac{K'}{K} + \varepsilon_0 \varepsilon_p \frac{h}{a} \tag{6}$$

B. Microfabrication Process

Fabricating sensors from materials currently used in orthopedic components has several advantages. Developing fabrication systems which use materials currently approved by the Food and Drug Administration reduces concerns of approval and biocompatibility. Furthermore, fabricating

sensors on the polyethylene insert material results in a new device which is substantially equivalent to existing devices from a functional perspective. In order to optimize capacitor response, the sensor material's elastic modulus should match the sensing material compliance as closely as possible. Fabricating the sensor using the implant material reduces concerns of compliance matching. Fig. 4 displays an overview of the fabrication steps.

The parallel plate capacitor in Fig. 2 is 610 micrometers square. The shear sensors are 1 millimeter by 300 micrometers wide with 20 micrometer gaps between the bottom electrodes. The interdigitated capacitors represent the most challenging structures from a fabrication standpoint. The overall dimensions of the sensor are 1,100 by 250 micrometers; however, the legs are 5 micrometers wide with 2 micrometer gaps between them. For the polyethylene adhesion experiments, a series of electrodes was fabricated with minimum feature sizes ranging from 2 to 5 micrometers to determine the minimum feature size achievable using this process.

The primary material used in the bearing between the femoral and tibial components is ultra-high molecular weight polyethylene (UHMWPE). Polyethylene is a low surface energy material, which makes the application of coatings challenging. Early attempts to fabricate electrodes on this surface were not successful. A rigorous cleaning and activation process was developed which enabled the successful deposition of electrodes on substrates made of polyethylene. This cleaning process consisted of an initial rinse in 5% liquinox and deionized water solution while gently scrubbing with nitrile gloved fingers. Liquinox cleaning was followed by rinsing with acetone, followed by methyl alcohol, and a final ethyl alcohol rinse.

Two substrates were used for polyethylene fabrication experiments, a 4.0 inch diameter 1.0 mm thick commercial, high-density polyethylene sheet material and a 3.0 inch diameter 4.5 mm thick compression molded medical-grade UHMWPE disk.

Following the primary cleaning, substrates were exposed to oxygen plasma using an Oxford Plasmalab 80+. The pressure during etching was $5x10^{-4}$ Torr. The RF power and frequency were 150 Watts and 13.56 MHz. Flow rates of 50 standard cubic centimeters (sccm) of O_2 and 4 sccm of N_2 were used to clean and activate the surface. The substrates were exposed to the plasma for 20 seconds.

Following cleaning, electrodes were patterned on the surface using the image reversal photolithography technique. Samples were coated with positive Shipley S1818 photoresist using spin-casting techniques. The substrates were soft-baked in an oven at 90° C for 30 minutes and subsequently exposed to ultraviolet light with a Hybrid Technology Group (HTG) system III-HR contact alignment system. Following exposure, wafers were baked for 90 minutes in a Yield Engineering Systems model 58SM image reversal oven containing an ammonia environment. Ammonia gas in the oven reacts with the acids in the exposed resist, yielding exposed areas insoluble in photoresist developer (thus reversing the initial exposure). Subsequent to baking in the image reversal oven, the substrate was flood exposed for 60 seconds which renders the originally unexposed material soluble to the developer. Samples were developed in Shipley MIF 321 for 60 seconds. The lower level of electrodes was applied using electron beam evaporation. 100 angstroms of titanium followed by 200 nanometers of gold was deposited on the substrates. Unwanted gold was "lifted-off" the substrate by stripping the photoresist in Shipley 1165 solvent.

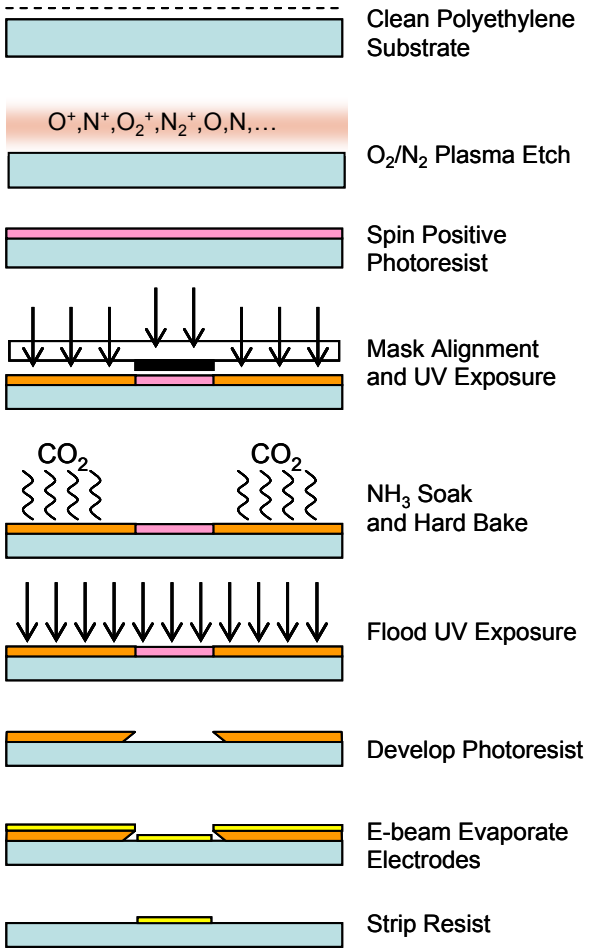

Fig. 4. Processing steps for fabricating gold electrodes on polyethylene substrate.

Parylene C was used as the dielectric layer. Parylene C has been used in several FDA-approved medical devices, such as drug-delivery stents and pace maker components. The parylene deposition process is a conformal, thin-film process resulting in a polymer layer with a dielectric constant of 3.

Vias were patterned in the parylene dielectric layer by patterning in photoresist followed by oxygen plasma

etching. A similar photolithography, image-reversal, electron beam evaporation, lift-off process was used for the upper electrode patterning.

III. Results

Following surface activation the polyethylene samples were examined with a Phase Shift Technologies ADE Phase Shift optical interference profilometer. The effects of the surface treatment of the polymer substrates are illustrated in Fig. 5. Increased numbers of small features are visible in the plasma treated sample Fig. 5b as compared to the untreated sample in Fig. 5a.

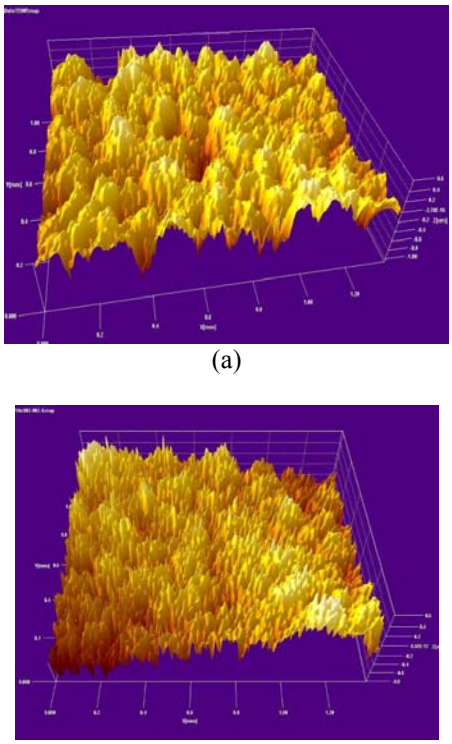

(a)

(b)

Fig. 5. 1.2 x 1.2 mm optical profilometer scans of polyethylene substrates. Fig. 5a is of untreated polyethylene surface. Fig. 5b is of Oxygen/Nitrogen plasma treated surface.

The surface of the polymer is activated when some of the polymer chains are broken or some of the hydrogen atoms are lost from the polymer backbone. These sites are locations where oxygen atoms and nitrogen atoms or hydroxyl groups may attach to functionalize the surface. This results in more polarized atoms on the surface increasing the energy of the surface. The results are seen in greatly improved adhesion of deposited materials during lithography steps. Prior to activation of the surface, no material remained on the polyethylene samples following metal deposition and lift-off. Using an oxygen plasma containing a flow of 2% Nitrogen we were able to increase the energy of the polyethylene surface such that 2 micrometer features were obtained.

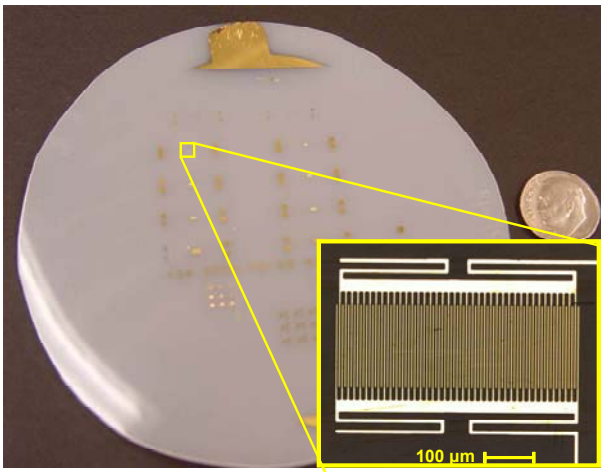

Fig. 6. Example of interdigitated capacitive sensors fabricated on polyethylene substrates. Inset is image of interdigitated electrode with 5 micrometer fingers and 2 miicrometer gaps between legs.

IV. Conclusion

A sensor array has been designed that will allow for the full characterization of stress and strain in three dimensions. Devices have been fabricated using a process incorporating fully-biocompatible materials, and the biocompatible polymer parylene has been patterned using photolithography and RIE to produce patterns of polymer features. We are currently developing application-specific integrated circuits to measure the small changes in capacitance produced by these sensors and testing the fabricated sensors. These biocompatible sensing systems will give researchers a better understanding of the kinetics and kinematics of orthopedic implants and enhance their performance both globally in design and individually through patient-specific *in vivo* evaluation.

References

[1] National Hospital Discharge Summary 2001. National Center for Health Stats. Available: http://www.cdc.gov/nchs/data/series/sr_13/sr13_156.pdf

[2] JA Rodriguez, H Bhende H, CS Ranawat. Total Condylar Knee Replacement A 20-Year Followup Study. Clin Orthop 388: 10-17, 2001.

[3] DR Diduch, JN Insal, WN Scott, GR Scuderi, D Font-Rodriguez. Total Knee Replacement in Young, Active Patients. Long-Term Follow-up and Functional Outcome. *J Bone Joint Surg Am*. 79:575-582, 1997.

[4] NW Rydell. Forces acting on the femoral head-prosthesis. A study on strain gauge supplied prostheses in living persons. *Acta Orthop Scand.* 1966;37:Suppl 88:1-132

[5] G Bergmann, F Graichen, and A Rohlmann, N Verdonschot, GH van Lenthe. Frictional heating of total hip implants. Part 1. measurements in patients. Journal of Biomechanics 34;421-428, 2001..

[6] DD D'Lima, S Patil, N Steklov, JE Slamin, CW Colwell, Jr. Tibial Forces Measured *In Vivo* After Total Knee Arthroplasty. *J Arthroplasty*, vol. 21 no. 2, pp. 255-262, 2006.

[7] H Ishikawa H, H Fujiki, K Yasuda. Contact Analysis of Ultrahigh Molecular Weight Polyethylene Articular Plate in Artificial Knee Joint During Gait Movement. (1996): *J. Biomech. Eng.* 118, pp. 377-386.

[8] J Liau, C Cheng, C Huang, and W Lo. Effect of Fuji pressure sensitive film on actual contact characteristics of artificial tibiofemoral joint. (2002): *Clin. Biomech.* **17** pp. 689-704.

[9] MR Mahfouz, WA Hoff, RD Komistek, and DA Dennis. A robust method for registration of three-dimensional knee implant models to two-dimensional fluoroscopy images. (2003) *IEEE Trans. Med. Imaging* 22: pp. 1561-1574.